Cavity ringdown laser absorption spectroscopy and time-of-flight mass spectroscopy of jet cooled platinum silicides

J. B. Paul, J. J. Scherer,[a] C. P. Collier, and R. J. Saykally
Department of Chemistry, U.C. Berkeley, California 94720

(Received 19 June 1995; accepted 15 November 1995)

The cavity ringdown technique (CRLAS) has been employed to measure the gas phase absorption spectrum of the platinum silicide molecule in the 350 nm region. All nine of the measured rovibronic bands are assigned to a single $^1\Sigma - ^1\Sigma$ electronic transition, with a ground state vibrational frequency of $\omega_e'' = 549.0(3)\ \mathrm{cm}^{-1}$, and a bond length of $r_0'' = 2.069(1)$ Å. The results of this study are compared with experimental data for the coinage metal silicides. Additionally, time-of-flight mass spectrometric results indicate that a variety of polyatomic metal silicides are formed in our molecular jet expansion. © *1996 American Institute of Physics.* [S0021-9606(96)01508-7]

INTRODUCTION

Compared with other transition metal silicides, platinum silicides have found by far the most success in state of the art, practical applications. To date, common uses for Pt–Si thin films are as robust, low resistivity contacts and interconnections in silicon-very large scale integrated (Si-VLSI) circuitry, and as Schottky barrier devices for use in infrared detectors and high resolution infrared CCD cameras.[1] Current research on PtSi has focused primarily on thin film growth mechanisms and their associated properties at the PtSi/Si interface. For example, it has been known for some time that when a thin film of platinum is deposited onto a silicon substrate and annealed, the Pt_2Si phase appears first, with the formation of the PtSi phase delayed until all of the free platinum has been incorporated as Pt_2Si.[2] Also clear in these early studies was that platinum is primarily the diffusing species during the formation of the Pt_2Si phase. However, many conflicting reports have been published concerning the diffusion kinetics during the PtSi growth phase. Recent studies undertaken to address this question present strong evidence indicating silicon is the predominantly mobile species during this phase.[2–4]

The study of molecular clusters is generally regarded as a possible route to understanding many solid state properties, such as those mentioned above. To our knowledge, however, no *ab initio* or gas phase spectroscopic studies of platinum silicide clusters have been reported. A large number of other platinum containing diatomic molecules have recently been investigated experimentally, including PtS,[5] PtC,[6] PtN,[7] PtO,[8] and Pt_2.[9] In this article, following our recent work on the coinage metal silicides (MSi, where M=Cu, Ag, Au),[10–12] we present the results of a study of jet-cooled platinum silicide clusters using cavity ringdown laser absorption spectroscopy (CRLAS) and time-of-flight mass spectroscopy (TOFMS), including the first spectroscopic characterization of the gas phase diatomic PtSi molecule.

EXPERIMENT

The Berkeley CRLAS spectrometer used in these experiments has been described in detail elsewhere.[10,13] The cavity ringdown method is based upon the measurement of the intensity decay rate of a light pulse trapped between two highly reflective mirrors. The small amount of light transmitting through one of the mirrors is recorded as a function of time, and fit to the following first order exponential expression:

$$I(t) = I_0 e^{-Lct/2l}.$$

From this, the total roundtrip cavity losses (L, due to mirror transmission, absorption, nonresonant scattering, etc.) can be easily calculated given the cavity length (l) and the speed of light (c). By subtracting the baseline losses, any frequency dependent absorption between the two mirrors can be detected with extremely high sensitivity (<1 ppm absorption per single pass). Typical reflectivities for mirrors in the visible region are on the order of 99.99%, giving ''ringdown times'' of tens of microseconds for a 0.5 m cavity, although reflectivities used in this (uv) study ranged from 99.7%–99.9% ($\sim 3\ \mu$s ringdown times). This rather low reflectivity did not significantly affect the results of this study as the signal was generally quite strong, such that the S/N ratio was good regardless of the sensitivity loss incurred due to the relatively poor mirrors.

The laser vaporization-supersonic cluster source employed in this work is similar to the design developed by Smalley *et al.*[14] with the main difference being that in our design the vaporization laser enters the source through the molecular beam exit channel, rather than through a separate channel. The vaporization target consisted of a 0.5 in. aluminum rod wrapped tightly with 0.012 in. platinum wire, which was glued in place and sanded to a smooth finish. This design was found to produce relatively stable cluster production while reducing costs compared with obtaining a platinum rod. The silicon was introduced into the source by mixing pure helium and a separate mixture of 2% SiH_4 in helium through a needle valve, allowing the concentration of SiH_4 entering the source to be controlled *in situ*. Optimal

[a]Current address: Sandia National Laboratories, Combustion Research Facility, Livermore CA 94551.

 0021-9606/96/104(8)/2782/7/$10.00

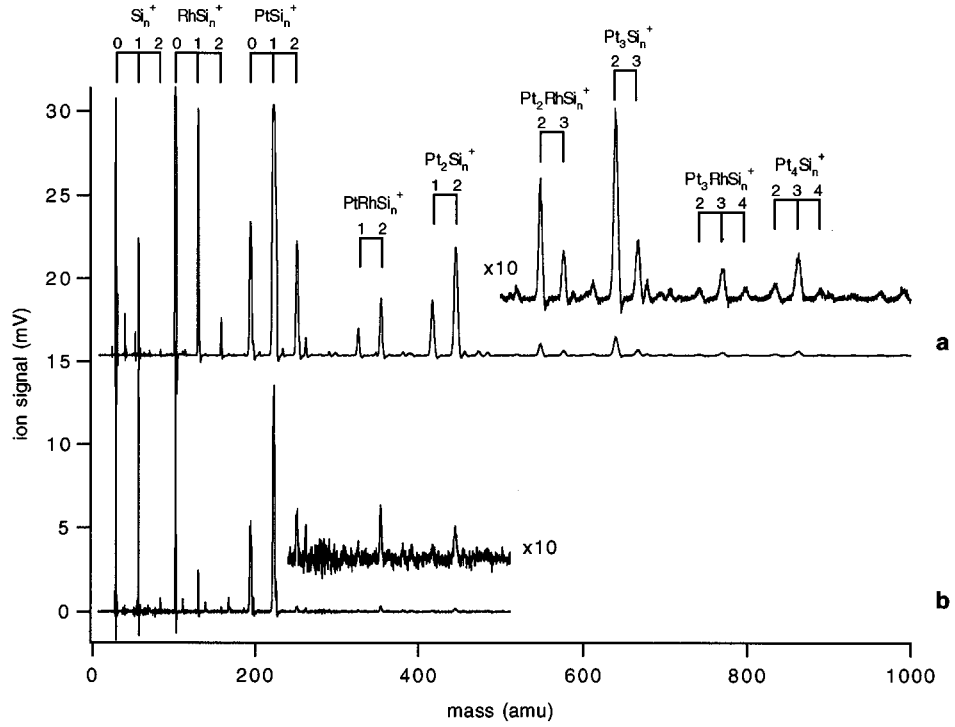

FIG. 1. TOFMS of platinum and rhodium silicides. Upper trace (a) is obtained with (Nd:YAG) 355 nm ionization, while lower trace (b) is observed with focused (excimer) 248 nm radiation. See the text for details.

SiH_4 concentration for these experiments was estimated to be ~0.5% in helium. Increasing the concentration was found to increase the noise level, due primarily to optical scattering from large silicon clusters produced in the molecular beam, whereas decreasing the concentration caused a noticeable decrease in the absorption signal intensity. Vaporization of the platinum was accomplished with either 80 mJ from a Nd:YAG laser operated at 355 nm, or 140 mJ from a 248 nm excimer laser, in both cases focused to a spot size of ~1 mm. A General Valve Series 9 pulsed valve delivered 80 psi of the carrier gas–silane mixture to the vaporization region. To reduce the noise level caused primarily by periodic fluctuations in our molecular beam source, 16 laser shots were averaged per wavelength step and up to 6 complete scans were averaged together. Laser frequency calibration was accomplished by measuring the known spectra of Al_2[15] (which is easily obtained by substituting an aluminum rod into the laser vaporization source) allowing an absolute wavenumber accuracy of 0.2 cm^{-1}.

Two different source tip extensions were used in this study. The first was a fan shaped nozzle described in our previous metal–silicide publications.[10–12] This design, while increasing the absorption path length and very effectively producing large numbers of PtSi clusters, was ineffective at cooling them rotationally. Rotational temperatures measured using this nozzle were typically ~200 K. In general, the addition of impurities into the monatomic carrier gas is found to increase the rotational temperature of molecules formed in the expansion. A simple cylindrical nozzle (2 mm diameter, 1 cm long) was substituted for the fan shaped nozzle in order to more effectively cool these clusters. To provide still additional cooling, argon was substituted for helium in the carrier gas. Rotational temperatures achieved with this configuration were typically ~40 K. While the absorption signal was not as strong, the cooler temperatures served to simplify the spectra, particularly in the band origin regions.

Attached to our CRLAS spectrometer is a time-of-flight mass spectrometer, which allows us to monitor cluster production while simultaneously scanning the ringdown spectrometer. This portion of the apparatus has also been previously described in detail.[10] Ionization of the neutral clusters was accomplished with either 355 nm (3.5 eV) or 248 nm (5.0 eV) radiation. Typically 1000 shots were averaged for each mass spectrum.

RESULTS AND ANALYSIS

TOFMS

The time of flight mass spectra in Fig. 1 show the presence of a variety of platinum silicide clusters in our molecular beam. The upper spectrum (a) was obtained with 355 nm ionizing radiation (100 mJ/cm^2), while the lower (b) was observed with 248 nm ionization (500 mJ/cm^2). Also apparent in these spectra are peaks due to a 20% rhodium impurity in the platinum wire. The largest cluster observed is $Pt_5Si_4^+$, with the largest peaks for $Pt_mSi_n^+$ in general occurring when $m=n+1$ for $m>2$, and when $m=n$ for $m=1$ or 2. It is not

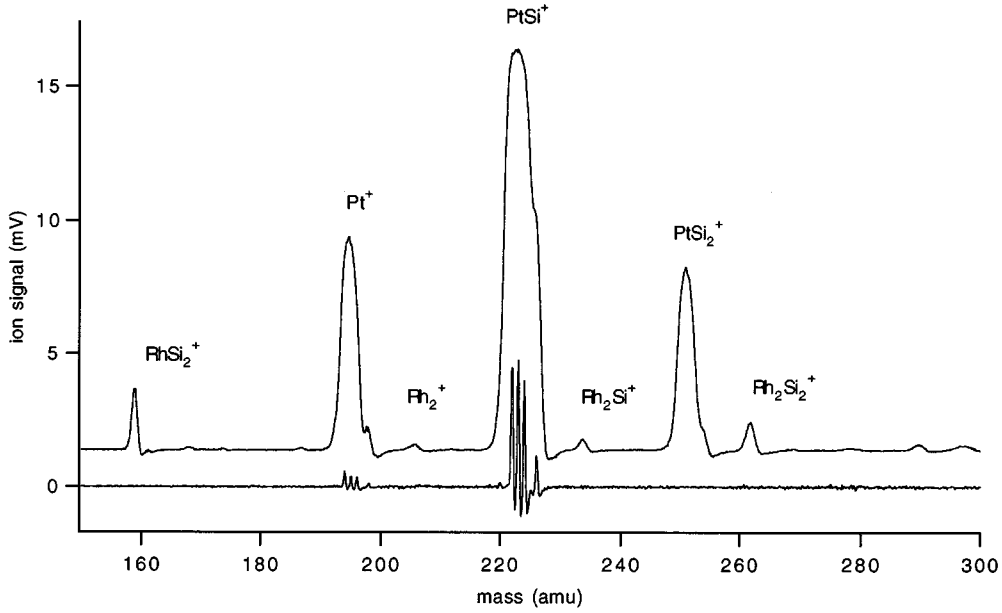

FIG. 2. Comparison TOFMS obtained via 355 nm (upper) and unfocused 248 nm (lower) ionization. Notice the pronounced loss of resolution in the upper trace, presumably due to photofragmentation effects.

clear whether this reflects a relative stability in the parent cluster or in the fragment (or both). Additionally, it appears that a single Rh substitutes readily for a Pt in the silicide clusters, evidenced by the large $Pt_nRhSi_n^+$ peaks, which maintain a very consistent ratio with the counterpart $Pt_{n+1}Si_n^+$ peaks.

The spectral features in the 355 nm spectrum appear significantly broadened compared with the 248 nm spectrum (Fig. 2). The upper trace in this figure is a blowup of the spectrum in Fig. 1(a). In the lower trace, the fluence of the 248 nm radiation has been reduced to 40 mJ/cm^2, and the only peaks observed are the Pt^+ and $PtSi^+$ peaks shown in the figure. This line broadening is most likely a consequence of parent molecule dissociation, which is commonly a result of multiphoton ionization (3 photons for 355 nm vs 2 for 248 nm). Additionally, the line broadening observed when the 248 nm laser fluence is increased [Fig. 1(b)] also suggests increased photofragmentation.

The $PtSi^+$ signal is the largest signal for any platinum-containing cluster. The fact that the 0–1 vibronic band of the PtSi system investigated here (see below) falls at 355.5 nm allows the possibility that this is the result of a resonant enhancement, except that this same $Pt^+/PtSi^+$ ratio is observed for both the unfocused and focused cases using 248 nm ionization. In light of this, PtSi may actually be the most abundant species in our molecular beam, consistent with the strong absorption signal measured with our CRLAS spectrometer. Due to the obvious problems involved in interpreting spectra obtained from multiphoton ionization, no further analysis of this data will be presented here.

CRLAS

Spectra of platinum silicide were observed in the same region (340–400 nm) where spectra of other metal silicides have recently been measured.[10–12] The PtSi bands measured in this study are some of the strongest molecular transitions ever measured with our molecular beam apparatus. In fact, when using the fan-shaped nozzle, the intensities of the heads of many of the bands could not be accurately measured, due to the fact that for such a strong absorption the entire ringdown decay occurred within the rf noise produced by the firing of the excimer laser ($\sim$1 μs). In these cases, we estimate the true molecular absorption to be on the order of 1% *per pass* of the probe laser.

Vibrational analysis

A total of nine bands have been assigned to transitions from the molecular ground electronic state to a single excited electronic state. Low resolution (0.3 cm^{-1}) spectra of several of these bands are shown in Fig. 3. A list of bandhead frequencies with vibrational assignments is given in Table I. Therefore, due to a lack of high reflectance mirror coverage, wavelengths below $\sim$337 nm were inaccessible. Thus bands beyond the (2–0) could not be measured despite the fact that this band was the strongest measured. Since not all of the bands could be rotationally analyzed to determine the exact origin positions, the bandhead frequencies were used to determine the vibrational constants. In the ground state, the first three vibrational levels appear well behaved, giving $\Delta G_{1/2} = 545.1$ cm^{-1}, and $\Delta G_{3/2} = 541$ cm^{-1}. For the reasons

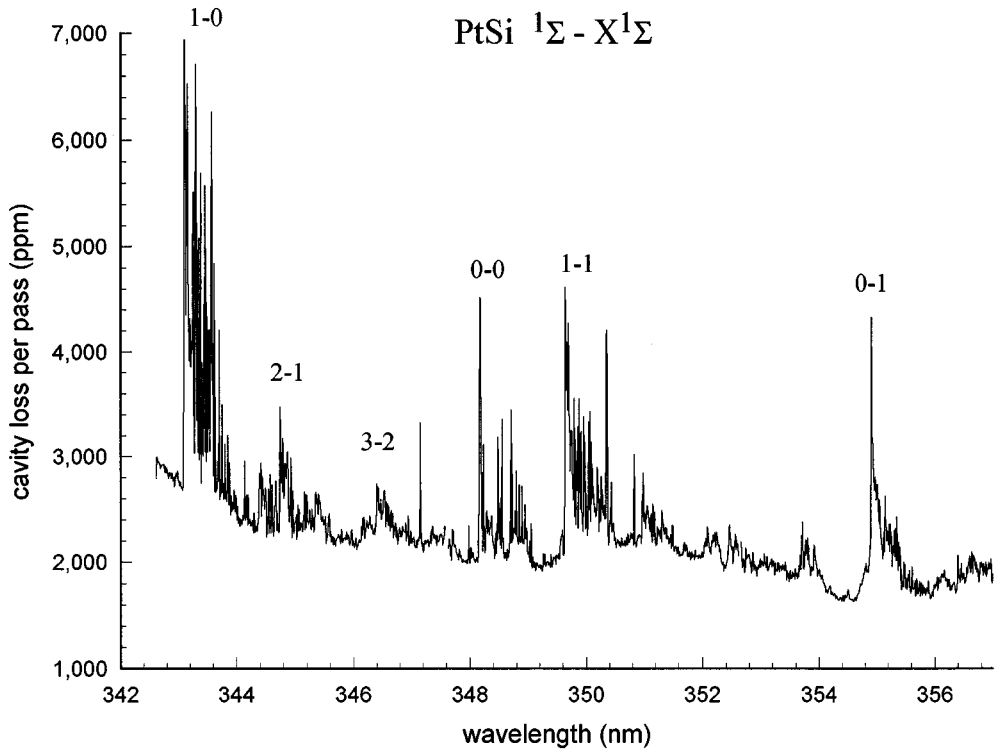

FIG. 3. Low resolution (0.3 cm^{-1}) CRLAS spectra of PtSi, showing many of the bands measured in this work. The intensities of the bands shown here are distorted because the large wavelength step size (0.01 nm) used to obtain this spectra caused the laser to miss the peaks of many of the spectral lines. For example, the intensity of the 0–0 band is found to be nearly twice that of the 1–1, even though they appear to have similar intensities in this scan.

given below, these vibrational levels were fit independently from the upper state levels using the following expression:

$$\nu = \nu_0 + \omega_e''(v''+1/2) - \omega_e\chi_e''(v''+1/2)^2,$$

yielding $\omega_e'' = 549.0(3)$ cm^{-1} and $\omega_e''\chi_e = 1.9(1)$ cm^{-1}. The three measured upper state vibrational intervals (425, 406, and 403 cm^{-1}) clearly do not fit to a quadratic expression. It should be noted that of the nine bands measured, only the (3–2) terminates in the $v' = 3$ level of the upper electronic state. While this band is reproducible, it is too weak to rigorously assign to this system through rotational analysis. Thus it is remotely possible that this band does not belong to the same system as the others. Due to the limited number of upper state vibrational levels measured, and the fact that they do not fit to the standard second order expression, we report only $\Delta G_{1/2}$ for the upper state. These constants are listed in Table I.

TABLE I. Bandhead positions of the PtSi bands measured in this study.

Assignment ($v'-v''$)	Bandhead frequency (cm^{-1})
0–2	27 635.1
1–2	28 059.5
0–1	28 176.2
1–1	28 600.8
0–0	28 721.3
3–2	28 869.5
2–1	29 007.1
1–0	29 145.9
2–0	29 552.5

Both the vibrational assignment and the spectral carrier are verified by the observed vibrational isotope shifts (see, e.g., Ref. 10). The four naturally abundant isotopes of platinum (masses 194, 195, 196, and 198 amu, occurring in the ratio 33:34:24.5:7.5, respectively), combined with the single abundant Si isotope, predicts a fourfold splitting of the spectrum with the intensity ratios given by those of the platinum isotopic abundance. Figure 4 shows a portion of a high resolution scan of the (2–0) band, showing an average shift of 0.235 cm^{-1} between adjacent masses, which is very close to the calculated value for PtSi of 0.234 cm^{-1} (assuming the rotational isotope effect is negligible). Bands arising from the two less abundant isotopes of silicon (^{29}Si, 4.7% and ^{30}Si, 3.1%) are also observable, yet are weak and were not analyzed.

Rotational analysis

The measured bands all have the characteristic appearance of a $^1\Sigma - ^1\Sigma$ transition, and were fit to the expression appropriate for this type of transition, given by,

$$\nu = \nu_0 + B'J'(J'+1) - B''J''(J''+1).$$

Of course, many types of electronic transitions can result in bands with this appearance, which are considered briefly in

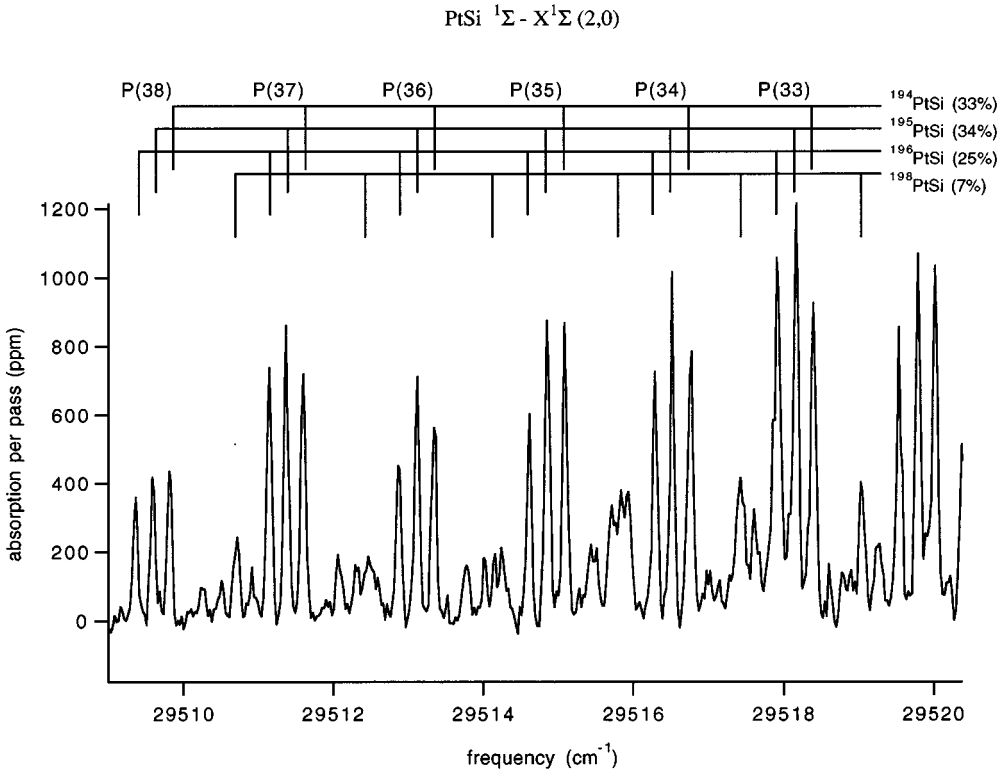

FIG. 4. High resolution (0.04 cm^{-1}) CRLAS spectra of *P*-branch lines of the 2–0 vibronic band of the PtSi system measured here. Each line is split into four components by the vibrational isotope effect, allowing the unambiguous assignment of this system. Most of the lines not labeled are due to the *R* branch.

the following section. Despite the simple nature of these bands, the location of the origin gap could not be easily determined. In the cases of the (0–0) and (1–0) bands, this resulted from the fact that *R* branch lines returning from the bandhead happen to fall directly on top of the *P* branch lines [Fig. 5(a)], causing a line to appear exactly at the band origin. For the remainder of the bands, the origin gap was obscured by spectral congestion resulting from the vibrational isotope shifts. While this prevented a completely rigorous determination of the rotational assignment, the results of band simulations [Fig. 5(b)] and comparisons with other molecules (particularly PtS,[5] PtC,[6] and AuSi[12]) strongly indicate the correct assignment is that which yields a ground state bond length (r_0) of 2.069 Å. Arguments in support of this assignment are presented below. In total, 30 lines were fit for the 0–0 band, and 35 were fit for the 1–1. Since the various isotopomers could not be resolved for these bands, the line centers were used in the fits. Thus these results should be closest to those that would be obtained for the ^{195}Pt isotopomer. Distortion constants were excluded from the fits as they were found to contribute insignificantly to the results, and therefore could not be accurately determined. A list of fitted line positions with residuals is available from the authors upon request. The results of this analysis are summarized in Table II.

DISCUSSION

The fact that none of the measured bands show *Q* branches, combined with the molecular orbital arguments presented below, lead us to assign these bands to a $^1\Sigma-^1\Sigma$ electronic transition. In support of this assignment, first consider the simple molecular orbital picture of the PtSi diatom. The Pt ^3D ground state arises from a $5d^9 6s^1$ atomic configuration, while the Si ^3P ground state results from a $3s^2 3p^2$ valence. Assuming that the molecular ground state is formed from ground state atomic levels, one might expect the Pt $6s$ electron to pair with the Si $3p\sigma$ electron, and the Pt $5d$ hole to combine with the Si $3p\pi$ electron, giving a $\cdots\sigma^2\sigma^2\sigma^2\pi^4\delta^4 \rightarrow {}^1\Sigma^+$ valence MO configuration. In general, the combination of a ^3D state and a ^3P state will give singlet, triplet, and quintet Σ, Π, Δ, and Φ states, which cannot be ruled out because of the possibility that the measured bands arise from an $\Omega=0^{\pm}-\Omega=0^{\pm}$ transition, and the fact that large the spin–orbit splittings are expected for Pt-containing compounds. Additionally, other configurations are possible if the PtSi ground state is not formed from ground atomic states.

While there are currently no *ab initio* studies of PtSi, analogies to this case can be drawn from the NiSi *ab initio* study of Shim and Gingerich.[16] Their Hartree–Fock-configuration interaction (HF-CI) and multiconfigurational

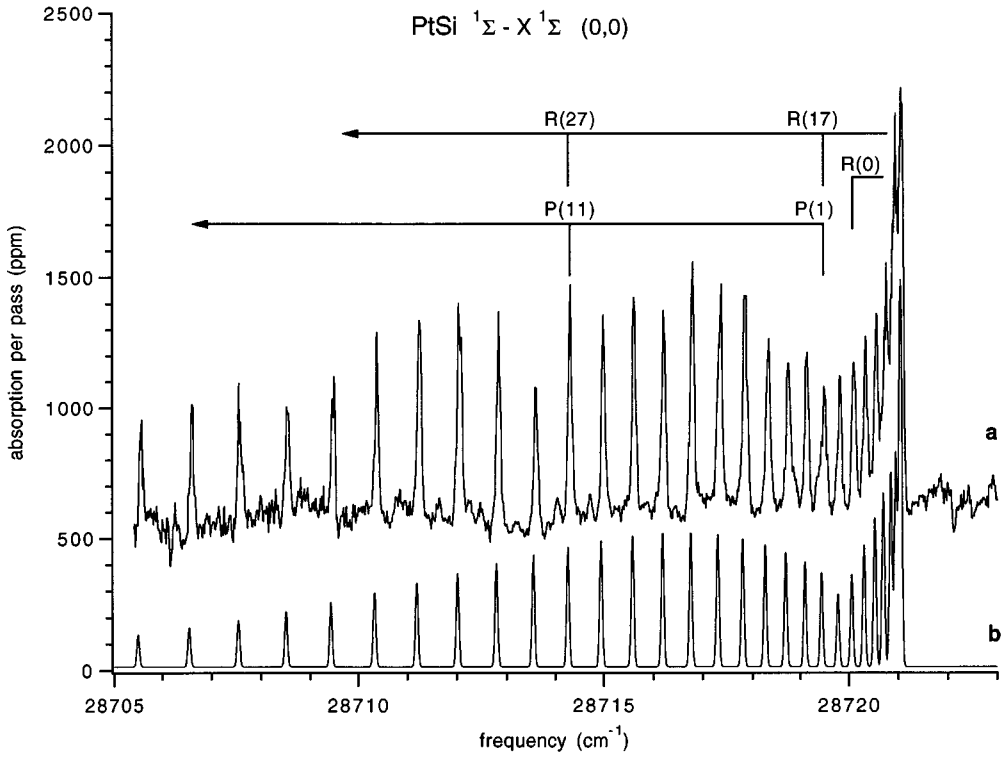

FIG. 5. (a) High resolution (0.04 cm^{-1}) CRLAS spectra of the origin band of the PtSi system measured in this study. (b) Simulation based on the B values reported in this study, and a rotational temperature of 40 K.

self-consistent field (CASSCF) calculations predict that the ground state of NiSi is formed when an electron in the Ni atom is promoted from the normally filled s shell in the atomic ground state configuration ($3d^8 4s^2$) into the d shell, giving a $3d^9 4s^1$ configuration (isovalent with atomic Pt ground state). Delocalized σ and π bonds are then formed by pairing the Ni $4s$ and Si $3p\sigma$ orbitals, and the Ni $3d\pi$ hole with the Si $3p\pi$ electron, resulting in a $9\sigma^2 10\sigma^2 11\sigma^2 4,5\pi^4 1\delta^4 \rightarrow {}^1\Sigma^+$ configuration. The fact that this is the same valence configuration naively given above reinforces the possibility that this description of the bonding in PtSi is correct. In this case, however, the extension of Pt $5d$ orbital beyond the $6s$ (not the case for the Ni $3d/4s$ orbitals) allows d-orbital bonding to play a more significant role,[17] which could explain the increased thermochemical well depth of PtSi[18] (5.1 eV) compared with that of NiSi[19] (3.2 eV).

TABLE II. Molecular constants of the PtSi system measured in this study.

Constant	$X\ ^1\Sigma$	$^1\Sigma$
ν_{00} (cm^{-1})	0	28719.8(4)
ω_e (cm^{-1})	549.0(3)	$\Delta G_{1/2}$=424.6(4)
$\omega_e\chi_e$ (cm^{-1})	1.9(1)	
B_0 (cm^{-1})	0.160 88(13)	0.143 01(13)
B_1 (cm^{-1})	0.159 86(13)	0.141 57(12)
r_0 (Å)	2.069(1)	2.195(1)

The rotational assignment given above is strongly supported by comparison with experimental results for PtS.[5] The bond force constant of PtS (4.92 mdyn/Å) is slightly larger than the PtSi force constant (4.31 mdyn/Å), where both values are obtained from the respective $\Delta G''_{1/2}$ values. It is therefore consistent for the PtS bond length of 2.042 Å to be slightly shorter than the 2.069 Å bond length derived from the given rotational assignment. If the PtSi band origin assignment is shifted one rotational line in either direction, the resulting bond lengths of 1.963 or 2.200 Å agree poorly with the PtS bond length.

The above description of PtSi is also consistent with experimental results for the isovalent PtC.[6] It is proposed that the PtC $^1\Sigma^+$ ground state arises from essentially the same valence MO configuration predicted for NiSi, and also proposed above for PtSi. The measured ground state bond length of 1.679 Å (for ^{195}PtC) is 0.390 Å shorter than the PtSi bond length. This difference is approximately equal to the difference between the covalent radii of Si and C (0.400 Å), supporting both the assumption that these two molecules share the same valence MO configuration, and the rotational assignment associated with this bond length.

Compared with the coinage metal silicides, the PtSi bond length decreases and the vibrational frequency increases considerably, resulting from a substantially increased bond strength.[10–12] This is shown in Fig. 5. Unlike the coinage metals, the platinum ground state open d shell is readily

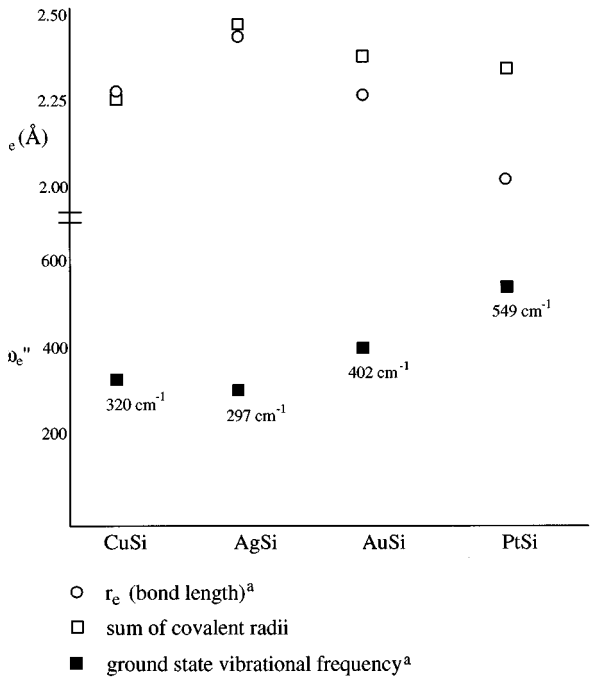

FIG. 6. Plot of the properties of all of the transition metal silicides measured thus far in our laboratory. (a) Values other than those for PtSi are taken from Refs. 10–12.

available for bonding. Clearly, these *d*-orbital contributions are responsible for the increased strength of this bond. This is particularly apparent when PtSi is compared directly with AuSi, as the valence of the constituent atoms of these molecules differ only by the *d* hole in the Pt. The double bond character of the PtSi bond predicted by the simple MO arguments above is reflected in the fact that the PtSi force constant (4.37 mdyn/Å) is nearly double that of 2.33 mdn/Å for AuSi. This dramatic increase in bonding is also observed when comparing Pt_2 with Au_2, where the significantly stronger Pt_2 bond is similarly ascribed to *d*-orbital interactions.[9]

CONCLUSIONS

Direct absorption rovibronic spectra of PtSi has been obtained via the CRLAS technique. Analysis of nine bands in the 350 nm region arising from a single electronic transition has yielded molecular properties for the ground and excited $^1\Sigma$ states. Si appears to bond substantially more strongly with Pt than with any of the coinage metals, consistent the solid state findings showing that Pt experiences less electromigration through Si than do the coinage metals.[20] This increase in bonding can be attributed to *d*-orbital interactions arising from the open Pt 5*d* orbital. Future experiments will focus on obtaining the spectra of polyatomic metal–silicides, which will hopefully further elucidate the solid state properties of these important compounds. *Ab initio* calculations would be of great value in this endeavor.

ACKNOWLEDGMENTS

This work was supported by the Air Force Office of Scientific Research (F49620-93-1-0278). Some equipment was provided by the National Science Foundation (CHE-9123335).

[1] T. L. Lin, S. D. Gunapala, E. W. Jones, H. M. Delcastillo *et al.*, IEEE Elect. Dev. Lett. **16**, 94 (1995); see also T. L. Lin, J. S. Park, S. D. Gunapala, E. W. Jones *et al.*, Jap. J. Appl. Phys. pt. 1, **33**, 2435 (1994); A. Akiyama, T. Sasaki, A. Mori *et al.*, Opt. Eng. **33**, 64 (1994); T. L. Lin, J. S. Park, T. George, E. W. Jones *et al.*, Appl. Phys. Lett. **62**, 3318 (1993); S. Uematsu, Vacuum **43**, 1039 (1992).
[2] J. E. McLeod, M. A. E. Wandt, R. Pretorius, and C. M. Comrie, J. Appl. Phys. **72**, 2232 (1992).
[3] Y. Kumagai, F. Hasegawa, and K. Park, J. Appl. Phys. **75**, 3211 (1994).
[4] D. X. Xu, C. J. Peters, J. P. Noel, S. J. Rolfe *et al.*, Appl. Phys. Lett. **64**, 3270 (1994).
[5] B.-Z. Li, K. Y. Young, and T. C. Steimle, J. Mol. Spectrosc. **170**, 310 (1995).
[6] T. C. Steimle, K. Y. Jung, and B.-Z. Li, J. Chem. Phys. **102**, 5937 (1995).
[7] E. J. Friedman-Hill, and R. W. Field, J. Chem. Phys. **100**, 6141 (1994).
[8] C. I. Frum, R. Engleman, Jr., and P. F. Bernath, J. Mol. Spectrosc. **150**, 566 (1991).
[9] S. Taylor, G. W. Lemire, Y. M. Hamrick, Z. Fu, and M. D. Morse, J. Chem. Phys. **89**, 5517 (1988).
[10] J. J. Scherer, J. B. Paul, C. P. Collier, and R. J. Saykally, J. Chem. Phys. **102**, 5190 (1995).
[11] J. J. Scherer, J. B. Paul, C. P. Collier, and R. J. Saykally, J. Chem. Phys. **103**, 113 (1995).
[12] J. J. Scherer, J. B. Paul, C. P. Collier, and R. J. Saykally, J. Chem. Phys. **103**, 9187 (1995).
[13] J. J. Scherer, J. B. Paul, and R. J. Saykally, in *Advances in Metal and Semiconductor Clusters*, Vol. III, edited by M. A. Duncan (JAI, Greenwich, 1995).
[14] D. E. Powers, S. G. Hansen, M. E. Geusic, D. L. Michalopoulos, and R. E. Smalley, J. Phys. Chem. **86**, 2556 (1982).
[15] Z. Fu, G. W. Lemire, G. A. Bishea, and M. D. Morse, J. Chem. Phys. **93**, 8420 (1990).
[16] I. Shim and K. A. Gingerich, Z. Phys. D. **16**, 141 (1990).
[17] S. P. Walsh and C. W. Bauschlicher, Jr., *Comparison of Ab Initio Quantum Chemistry with Experiment for Small Molecules* (Reidel, New York, 1985), pp. 17–51.
[18] A. Vander Auwera-Mahieu, R. Peeters, N. S. McIntyre, J. Drowart, Trans. Faraday Soc. **66**, 809 (1970).
[19] A. Vander Auwera-Mahieu, N. S. McIntyre, and J. Drowart, Chem. Phys. Lett. **4**, 198 (1969).
[20] S. Q. Hong, Q. Z. Hong, J. Li, and J. W. Mayer, J. Appl. Phys. **75**, 3959 (1994).